




Article

Modification of Microstructure and Mechanical Parameters of Austenitic Steel AISI 316L under the Action of Low Friction

Daria Grabco ¹, Olga Shikimaka ¹, Constantin Pyrtsac ^{1,2} , Daria Topal ¹, Dragisa Vilotic ³, Marko Vilotic ^{3,*}  and Sergei Alexandrov ^{4,5} 

- ¹ Institute of Applied Physics, Moldova State University, MD2028 Chisinau, Moldova; daria.grabco@ifa.md (D.G.); olga.shikimaka@ifa.usm.md (O.S.); constantin.pirtac@fiz.utm.md (C.P.); daria.topal@ifa.usm.md (D.T.)
- ² Faculty of Electronics and Telecommunications, Technical University of Moldova, MD2004 Chisinau, Moldova
- ³ Faculty of Technical Sciences, University of Novi Sad, Trg Dositeja Obradovića 6, 21000 Novi Sad, Serbia; vilotic@uns.ac.rs
- ⁴ Ishlinsky Institute for Problems in Mechanics RAS, 101-1 Prospect Vernadskogo, 119526 Moscow, Russia; sergei_alexandrov@spartak.ru
- ⁵ Department of Civil Engineering, Peoples' Friendship University of Russia (RUDN University), 6 Miklukho-Maklaya St, 117198 Moscow, Russia
- * Correspondence: markovil@uns.ac.rs

Abstract: This work is devoted to the study of the tribological properties of AISI 316L austenitic steel and the effect of the relative velocity of rubbing bodies on the microstructure and mechanical properties. The specificity of the deformation is investigated in the mode of dry friction “metal/metal”, namely, steel AISI 316L/steel St3sp, with a process duration of 15 h. The change in the microstructure of the samples as a result of friction and the determination of mechanical properties are carried out on the friction surface and on the cross-section of the samples. The mechanical parameters are studied by depth-sensitive indentation using a Berkovich indenter. It is shown that low friction with the relative velocity of rubbing bodies of about 30 rpm is capable of introducing noticeable microstructural and strength changes. Strength and relaxation properties (hardness, Young’s modulus, plasticity index, and resistance index) increase in samples subjected to friction compared to the original undeformed sample. A change in the microscopic structure of the samples near the friction surface increases such material properties as microhardness (H) and Young’s modulus (E). In particular, the microhardness increases from 1.72 GPa for the undeformed sample to 3.5 GPa for the sample subjected to friction for 15 h. Young’s modulus increases from 107 GPa to 140 GPa, respectively. A comparison with the properties of samples deformed at the relative velocity of rubbing bodies of about 300 rpm shows a further increase in the microhardness and Young’s modulus. Also noted is the sensitivity of the relaxation parameters to the friction process and the relative velocity of rubbing bodies. In particular, the relaxation parameters h_c and h_{res} decrease while h_{e-p} increases.

Keywords: AISI 316L steel; relative velocity of rubbing bodies; microstructure and mechanical parameters



Citation: Grabco, D.; Shikimaka, O.; Pyrtsac, C.; Topal, D.; Vilotic, D.; Vilotic, M.; Alexandrov, S. Modification of Microstructure and Mechanical Parameters of Austenitic Steel AISI 316L under the Action of Low Friction. *Metals* **2023**, *13*, 1278. <https://doi.org/10.3390/met13071278>

Academic Editor: Francisco J. G. Silva

Received: 20 May 2023
Revised: 9 July 2023
Accepted: 13 July 2023
Published: 16 July 2023



Copyright: © 2023 by the authors. Licensee MDPI, Basel, Switzerland. This article is an open access article distributed under the terms and conditions of the Creative Commons Attribution (CC BY) license (<https://creativecommons.org/licenses/by/4.0/>).

1. Introduction

Various machines, machine tools, instruments, and equipment necessarily consist of many components permanently in contact with each other while subjected to friction stress of greater or lesser intensity. As a result, the components wear out, affecting the performance quality and the product’s overall durability. For this reason, the study of various fundamental and applied aspects of the friction mechanism is very important, and a vast amount of the literature was devoted to these aspects [1–4]. In most cases, the regularities of deformation and the mechanism of the friction process are studied on materials and structures that are used in the creation of all kinds of moving parts and

machines. In [2], the authors thoroughly analyzed three FCC materials (aluminum, copper, and austenitic steel) using nanosliding and scratching at various load levels. A clear influence of mechanical parameters on the mechanism of deformation and wear was noted. The threshold values for the transition of the wear mechanism from sliding to scratching and chipping increased with increasing hardness in the Al-Cu-steel series. Along with this, the resistance index H^3/E^2 indicated the magnitude of the contact pressures, upon reaching which a change in the wear mechanism occurred.

The degree of wear depends not only on the properties of the material subjected to friction, but also on operating conditions such as normal forces, relative velocities, and the length scales of textured surfaces. The higher the values of these parameters, the more wear products appear, and this transforms the friction mode from adhesive to abrasive. Wang et al. [3] showed that, under dry conditions, the smoothest surfaces do not show the least friction from the increase in adhesion forces, as might be expected. A surface with a slight microstructure reduces the coefficient of friction. In turn, macro-textured surfaces markedly increase the coefficient of friction from the abrasive effect of the surface. The effect of deformation treatment of the surface of 40KhNMA steel during sliding friction on an abrasive surface was studied in [4]. It was shown that deformation treatment promotes an increase in size and the presence of bulk defects in the crystal structure of steel. Deformation treatment should be used to increase the hardness and bulk strength of 40KhNMA steel. To do this, it is necessary to use hardening, which simultaneously increases the resistance to plastic deformation and the destruction of steel, estimated by increasing the rheological parameter.

During friction, there is a rigid contact between two bodies, accompanied by the rising of significant inhomogeneity in local stresses near the contact surfaces. As a result, inhomogeneous plastic deformation occurs in materials subjected to friction. Bowden and Leben [5] found that the friction force does not remain constant between two pieces of metal moving relative to each other. The process of friction is not continuous but occurs in large jerks. Under the action of a normal force, the contacting surfaces seem to “stick together” to each other, and it is necessary to apply a tangential force for their relative movement. As a result of gradually increasing tangential stress up to a certain maximum value, a sudden and very fast sliding occurs. The tangential stress drops to zero at this instant until the relative motion stops again. Then the tangential stress begins to increase again, and the process repeats over and over. However, the nature of this process is not the same for various combinations of rubbing materials. On the one hand, the friction process depends on the physical properties of the rubbing materials (such as the chemical bond of rubbing materials, hardness, elasticity, melting temperature, etc.). On the other hand, the friction force and the nature of friction depend on external factors, such as the magnitude of the normal load acting on the rubbing surface, the temperature at which friction occurs, the presence of lubricants, the relative velocity of rubbing bodies, etc.

The presence of such a large number of factors affecting the mechanism of friction and wear, naturally, was the reason for numerous studies. For example, the authors of [6] used friction stir treatment (FSP) to harden the surface of AISI 440C high-carbon martensitic stainless steel. An increase in hardness up to 779 HV1 and higher than that of the conditionally hardened sample was achieved. In another work [7], in order to obtain a hardening effect in AISI 316L stainless-steel sheets, friction treatment with stirring was carried out at a constant speed (63 mm/min) and relatively low rotation speeds (200 and 315 rpm). It was found that despite the decrease in plasticity by 50%, the maximum yield strength and ultimate tensile strength of the samples processed by friction with stirring increased by about 1.6 and 1.2 times compared to the original metal. Dogan et al. [8] studied the issue of friction and wear of stainless steel implanted with nitrogen and zirconium and coated with TiN. These implantations have been shown to improve the coefficient of friction, as well as the wear resistance of the stainless-steel surface.

The effect of silicon carbide in the range from 35–200 μm at various normal loads ($P_{\text{norm}} = 50\text{--}110\text{ N}$) on wear of steel 35NCD16 microstructure and abrasive grains was

studied in [9]. It was shown that the coefficient of friction decreases with increasing normal load and/or decreasing abrasive particle size. At the same time, the wear rate increases with an increase in the normal load and/or abrasive particle size. It was found in [10] that severe abrasive wear occurs at low load, and the highest nanohardness, elastic properties, and creep resistance of SLMed IN718 superalloy is created directly under the wear surface. More detailed studies of various issues related to friction hardening were carried out by Rapoport and Rybakova [11,12], who established the formation of three microstructural levels (layers) near the contact surface.

The results above were confirmed in [13–15]. It was shown that during the friction of metal samples, the microstructure of a narrow surface layer differs significantly from that of the bulk since the material is subjected to ultrahigh internal stresses near the friction surface. These stresses are much higher than those in the bulk. In this case, a significant change in the material's behavior and the appearance of anomalous mass transfer phenomena naturally occur. It was also found that the length of the hardened surface layer depends both on the type of the deformable material (brass, copper, or steel) and on the friction method (hard dry friction, extrusion, impact, or indentation) [16,17].

From the reasons mentioned above that affect the specificity and degree of deformation during friction, it becomes obvious that the relative velocity of rubbing bodies also plays a significant role in all friction methods. This issue is studied insufficiently in the scientific literature and needs additional attention. In [17], the effect of friction on the micromechanical parameters of AISI 316L austenitic stainless steel was studied, taking into account the extensive use of this material in various sectors of the industry and, in particular, in medicine for manufacturing implants. In this work, the study of the specifics of deformation was carried out in two friction modes: 1—dry friction “metal/metal”, namely, steel AISI 316L/steel St3sp, and 2—dry friction “metal/abrasive”, steel AISI 316L/abrasive P2000, with different durations of the process ($t = 1; 5$ and 10 h). Friction processes were performed using a MoPao 160E grinding and polishing machine at a rotation speed of $v \approx 300$ rpm and a normal pressure of $P_{\text{norm}} \approx 400$ mN.

It was found that different modes of friction create plastic deformation in the test sample. The maximum modification of the microstructure was observed in a thin layer (≤ 100 μm) directly adjacent to the friction surface, i.e., in the zone of severe plastic deformation. The degree of plastic deformation successively decreased with distance from the friction surface, and the sample acquired the original polycrystalline structure at a distance of $t \approx 600$ – 700 μm . Along with this, a change in the mechanical parameters, such as microhardness (H), Young's modulus (E), plasticity index (H/E), and resistance index (H^3/E^2), also occurred. The degree of their change depended on the experimental conditions. Taking into account that the friction conditions, in particular the relative velocity of rubbing bodies, affected the microstructure and plasticity parameters noticeably, the study was continued at a lower rotation speed but a longer process time.

2. Materials and Methods

In the present work, the studies were carried out on AISI 316L stainless-steel specimens in the form of washers with a diameter of $\varnothing 15$ mm and height of 5 mm. This steel grade had the following chemical composition (in %): (C 0.019; Mn 1.74; P 0.017; S 0.001; Si 0.5; Cr 17.38; Ni 14.24; Mo 2.85; N 0.062; Cu 0.1; Fe 63.09). To carry out the friction experiment, the surfaces of the cut washers were prepared on a MoPao 160E polishing machine in several stages: dry polishing with abrasive paper (P 600, P 1500, P 3000), then wet polishing with Cr_2O_3 to a mirror finish in an optical microscope. The final surface roughness was $R_{\text{Sa}} = 16.24$ nm and can be considered a high-quality roughness (for comparison, we note that, in [18], shiny copper obtained by electrodeposition had a surface roughness $R_a = 0.613$ $\mu\text{m} = 61.3$ nm). All measurements were made on the prepared surface; then, the sample was subjected to chemical etching to reveal and study the grain structure. After that, the sample was cut perpendicular to the surface, and all stages of surface preparation and experiment were carried out similarly on the cross section. The specificity of deformation of

AISI 316L steel was investigated in the “metal/metal” dry friction mode, namely, AISI 316L steel/St3sp steel, with a process duration of 15 h. Friction was performed on a polishing machine. The axis of the specimen moves along a circle whose radius is 10 cm with a relative velocity of about 30 rpm. This velocity will be regarded as the relative velocity of rubbing bodies in what follows. The applied pressure was $P_{\text{norm}} \approx 400$ mN. The study of changes in the microstructure of samples as a result of friction and the determination of mechanical parameters were carried out on the friction surface and on the cross-section of the samples.

The study of mechanical properties (microhardness, Young’s modulus, plasticity index, and resistance index) was carried out by the method of depth-sensitive indentation on a Nanotester-PMT3-NI-02 device (Tambov State University, Russia) equipped with a Berkovich indenter at various maximum loads on the indenter in the range $P_{\text{max}} = (20\text{--}400)$ mN. The tests on the nanotester were carried out according to the following program: loading process for 20 s, exposure at a maximum load (P_{max}) for 30 s, and unloading for 20 s. For each load, 10 imprints were made. The results were calculated as the average value of 10 tests. Based on the analysis of the curves’ indentation, the main parameters of elasticity, plasticity, and strength were estimated. The calculations were carried out with the Oliver–Pharr method being extensively used in science [19]. All calculations were performed automatically using the instrument software.

The surface microstructure of the samples was studied by optical microscopy on Amplival (Carl Zeiss Jena, Germ.) and XJL-101 (TIME Group Inc., China) instruments with digital monitoring. Selective chemical treatment in order to reveal the grain structure was carried out in a solution of the composition: 2.5 mL HCl + 1 mL glycerol + 0.5 mL HNO₃, etching time $t_{\text{etc}} \approx 5$ min.

3. Results and Discussion

First, the microstructure of undeformed samples was studied. To do this, the samples were subjected to fine chemical polishing followed by selective chemical etching. As a result of the chemical treatment, it was found that the samples have a typical polycrystalline austenitic structure with a grain size in the range of (2–50) μm (Figure 1). It was also possible to note the different shapes and orientations of the crystallites, not only on the surface under study (Figure 1a) but also in the volume, on cross-sections (Figure 1b,c).

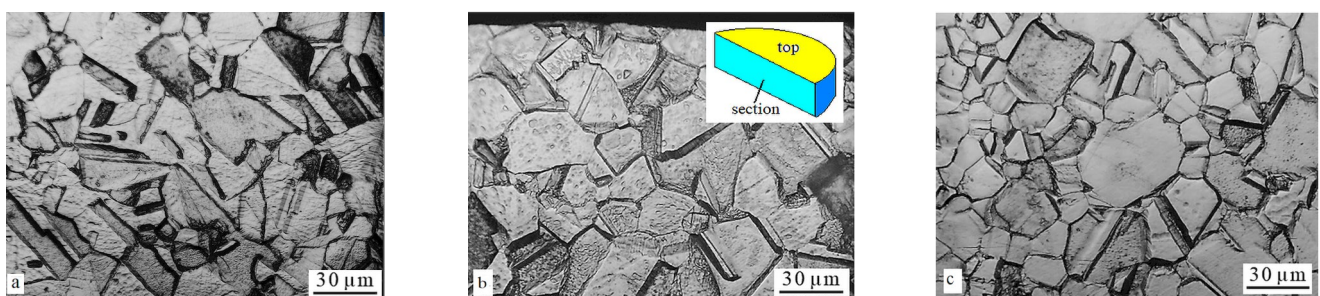


Figure 1. Microstructure of undeformed specimens after selective chemical etching. The top view (a); the view in section (b,c); the surface near the specimen’s edge (b); near the specimen’s center (c). A scheme added on (b) that illustrates the top view and sectional view of sample.

The studied samples were subjected to friction for 15 h. The microstructure and mechanical properties were determined on the friction surface (top view) and transverse sections of the samples (view in section) to reveal how deep the deformed zone extends into the depth of the sample. The microstructure at the friction surface with traces (strokes) from the rubbing materials, as well as three imprints made at $P = 400$ mN, are shown in Figure 2a.

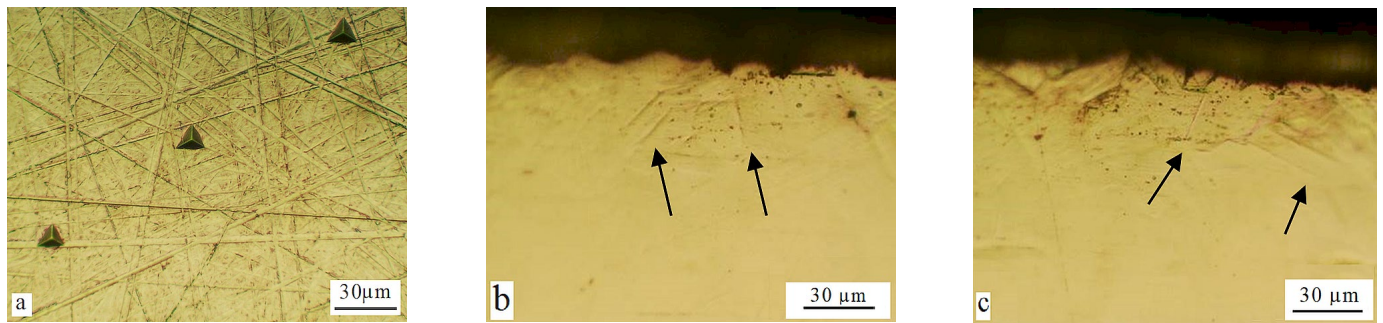


Figure 2. Microstructure after 15 h of friction and deformation slip bands at the load of $P = 400$ mN. The top view (a) and the view in section (b,c). The deformation slip bands extend into the sample for a depth of ≈ 50 μm (shown by arrows).

In Figure 2b,c, one can see slip bands that extend into the sample volume for about 50 μm . It should also be noted that the edge of the friction surface is not very even and smooth.

As further studies have shown, the irregularities are caused by the grain spalls at the intersection of several strokes, friction marks. This is clearly visible in Figure 3, showing an area with a smooth edge (Figure 3a), an area showing grain chipping (Figure 3b, marked with an arrow), and an area overcutting a thin layer of grain (Figure 3c, marked with an arrow). It can also be seen that the sample has a fine-grained structure away from the friction surface (≈ 500 μm) (Figure 3d–f). As they approach the friction surface (Figure 3a–c), the crystalline granules get smooth and coarse and become the same color, indicating their similar orientation. As the friction surface is approached [14], the deformation slip bands, which are formed as a result of the movement of dislocations, cross different grains, which leads to a smoothing of the boundaries between the grains and a decrease in their disorientation.

A change in the microscopic structure of the samples subjected to friction, as a result, led to a change in the main micromechanical characteristics, like microhardness (H) and Young's modulus (E). The change in H and E values on the friction surface as a function of the load on the indenter is shown in Figure 4. It can be seen that both parameters, with some fluctuations, experience a slight decrease with an increase in the load on the indenter from 20 to 400 mN. The effect was also seen in the cross-sections of both the undeformed (Figure 5a,b) and deformed specimens (Figure 5c,d). For comparison, three loads of 20, 100, and 400 mN were selected, which make it possible to estimate the hardness value in three ranges. In accordance with the literature data [20] and the international standard ISO 14577-1 [21], load $P = 20$ mN gives information about nanohardness, $P = 400$ mN refers to the microhardness range, and $P = 100$ mN is an intermediate load that binds nano and micro ranges. As follows from Figure 5, both strength parameters, H and E , for the deformed and undeformed samples demonstrate a regular decrease with increasing load by transfer from nanoindentation to microindentation.

On both samples in the nano-load region ($P = 20$ mN), an increase in the microhardness value is observed, known in the scientific literature as the indentation size effect (ISE) [22,23]. It is known that the size effect observed during indentation appears because of the influence of many factors: elastic recovery, dislocation-free crystal volume, grain size, surface roughness, etc. Considering that in our work the surfaces for research were prepared by polishing, it was important to check whether the final surface roughness does not affect the manifestation of this effect. The imprints made at $P = 10$ mN and 100 mN are shown in Figure 6. As follows from the figure, the relief of the undeformed surface in the vicinity of the imprint is negligibly small compared to the imprint depth. Since the surface roughness of the studied samples is $R_{\text{Sa}} = 16.24$ nm, the roughness will be 6.7% for the imprint of $P = 10$ mN and 4.6% for $P = 20$ mN. Thus, it can be assumed that the surface roughness does not significantly contribute to the manifestation of ISE during indentation

of AISI 316L steel. Rather, the influencing factors can be the elastic-plastic recovery of the imprint, grain size, dislocation interactions, material displacement to the surface in the form of a pile-up, etc. The measurements also showed that, on the cross-section of the deformed sample, as the distance from the friction surface increases, the hardness gradually decreases, and at a distance of $l \approx 500 \mu\text{m}$, it becomes equal to the hardness of the undeformed sample. The value of hardness, measured with a load of $P = 100 \text{ mN}$, varied as follows: $H = 3.75 \text{ GPa}$, 3.05 GPa , 2.43 GPa , and 1.82 GPa , respectively, for distances $l = 30 \mu\text{m}$, $100 \mu\text{m}$, $300 \mu\text{m}$, and $500 \mu\text{m}$ from the friction surface. Young's modulus experiences similar changes. The obtained data confirmed the results of work [17] for steel AISI 316L at 1, 5, and 10 h of friction.

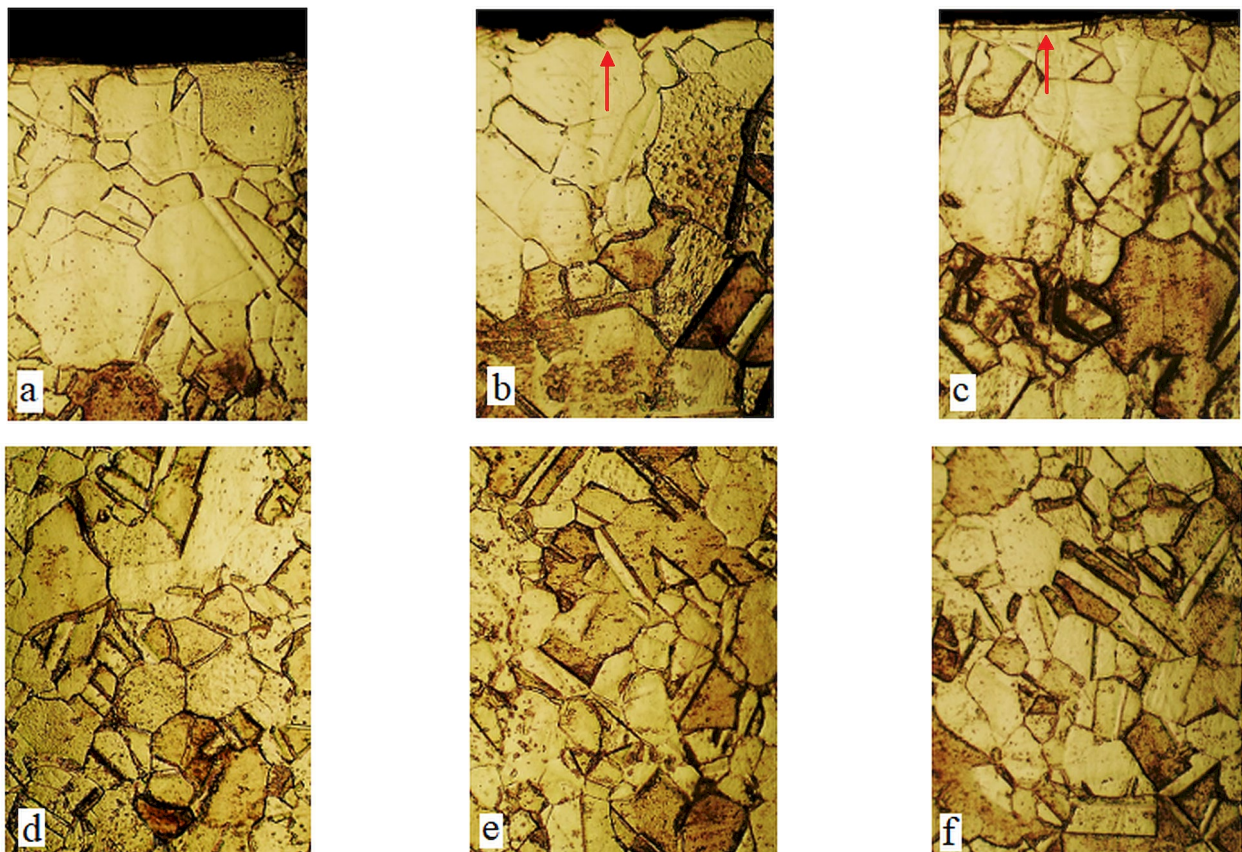


Figure 3. Microstructure after 15 h of friction followed by selective chemical etching, viewed in section. The surface microstructure near the friction surface of the sample (a–c); the microstructure at a distance of $\approx 500 \mu\text{m}$ from the friction surface (d–f). Image magnification of the horizontal side of each frame is $150 \mu\text{m}$.

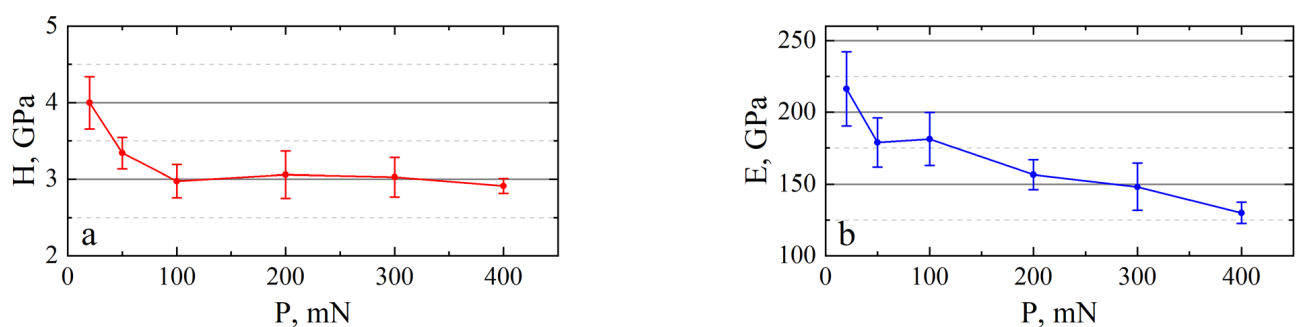


Figure 4. Top view. The dependence of the hardness (a) and Young's modulus (b) on the load after 15 h of friction.

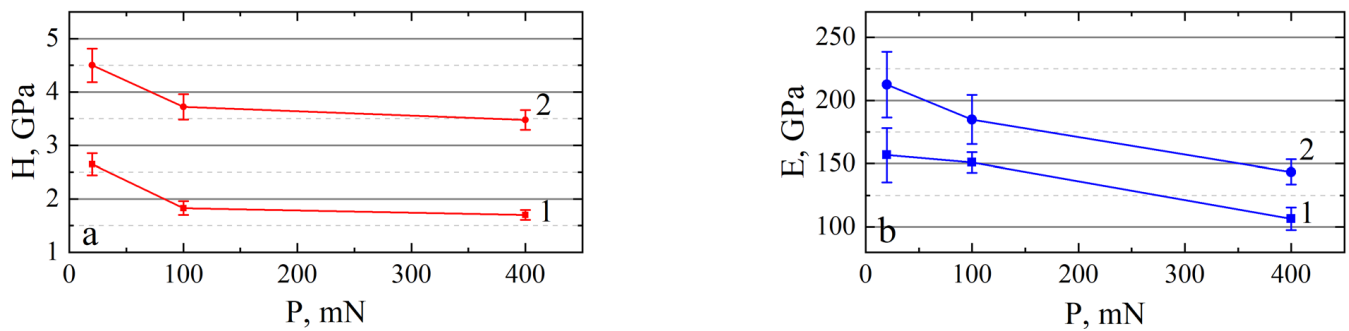


Figure 5. Effect of friction on the microhardness (a) and Young's modulus (b). Curves 1 correspond to the undeformed specimen (top view) and curves 2 to the cross-section at a distance of $l \approx 30 \mu\text{m}$ from the friction surface.

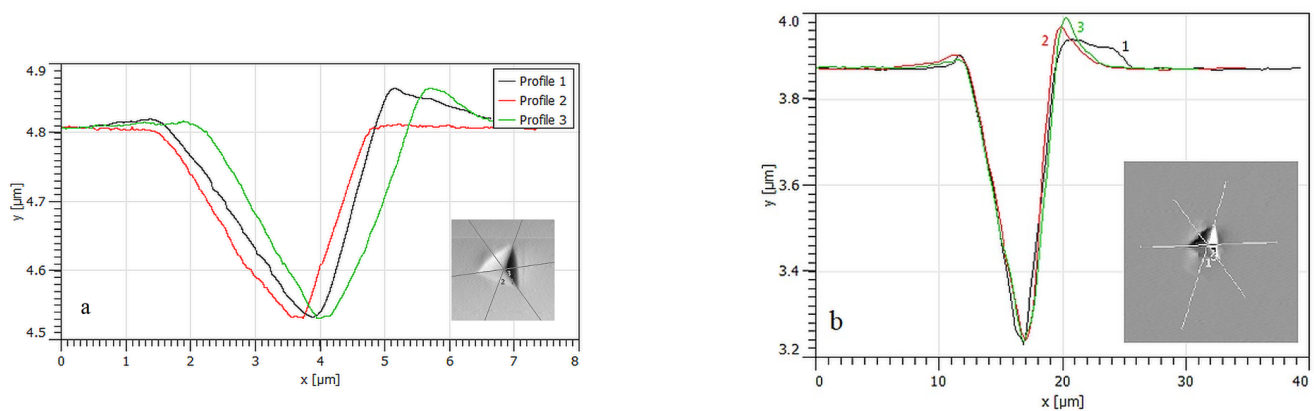


Figure 6. AFM. View of imprints in section; P , mN: (a)—10, (b)—100.

The change in the microhardness and Young's modulus results in a change in two other parameters, the plasticity index and the resistance index, which are estimated in the scientific literature as (H/E) and (H^3/E^2) , respectively [23–25]. They are important mechanical characteristics that determine the ductility and wear resistance of products during the operation. For example, the higher the H/E parameter, the lower the probability of brittle fracture, and the higher (H^3/E^2) , the higher the wear resistance. To evaluate the behavior of these parameters, let us compare their values for three types of samples: 1—undeformed sample; 2—sample deformed by friction ($v = 30 \text{ rpm}$, $P_{\text{norm}} = 400 \text{ mN}$, $t = 15 \text{ h}$ of friction); and 3—sample deformed by friction ($v = 300 \text{ rpm}$, $P_{\text{norm}} = 400 \text{ mN}$, $t = 10 \text{ h}$ of friction) and measured earlier in Ref. [17] (Table 1).

Table 1. Strength and plasticity parameters for different types of specimens.

Nr.	Sample	H , GPa	E , GPa	H/E	H^3/E^2 , GPa
1	Undeformed AISI 316L sample	1.72	107	0.016	$0.4 \cdot 10^{-3}$
2	Sample AISI 316L deformed at 30 rpm	3.5	140	0.024	$2.1 \cdot 10^{-3}$
3	Sample AISI 316L deformed at 300 rpm	3.68	160	0.026	$2.5 \cdot 10^{-3}$

As follows from the table, the values of all parameters of both deformed samples are significantly higher than the values of the undeformed sample. Moreover, the higher relative velocity of rubbing bodies ($v = 300 \text{ rpm}$) creates larger values of H , E , H/E , and H^3/E^2 compared to the velocity $v = 30 \text{ rpm}$. The results obtained can be useful for creating the materials with mechanical properties in accordance with their practical purpose, for

example, to combine high hardening with high ductility (H/E) or high hardening with high resistance to plastic deformation (H^3/E^2).

Along with this, another group of properties, namely relaxation parameters, is of great practical interest. Thus, the elastoplastic relaxation and recovery of imprints after nanoindentation must be taken into account in lithographic technologies that use printing (penetration of the resist marking with a pattern on a nanometer scale), recording and storing information by nanoindentation methods in memory devices, etc. [26].

The relaxation parameters of interest are the maximum imprint depth (h_{\max}), the indenter-sample contact depth at the maximum load without the elastic deflection of the surface (h_c), the elastic-plastic component of the indenter imprint, which is restored after complete unloading of the indenter, (h_{e-p}), and the residual depth of the imprint after the complete unloading of the indenter (h_{res}). These parameters are determined by analyzing the indentation curves $P(h)$ (Figure 7) [20,27,28]. Table 2 presents the relaxation parameters for the above three types of samples at a load of $P = 400$ mN. A characteristic feature of the given parameters is their sensitivity to the friction process and the relative velocity of rubbing bodies.

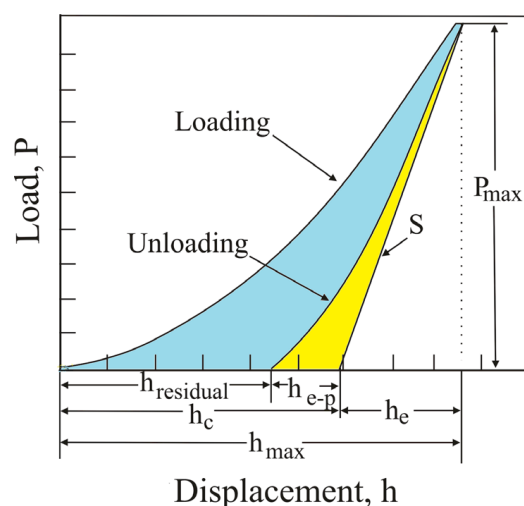


Figure 7. Typical diagram ‘loading-unloading’ $P(h)$, and the main relaxation parameters: h_{\max} , h_c , h_e , and h_{e-p} .

Table 2. Relaxation parameters for different types of specimens.

Nr.	Sample	h_{\max} , μm	$h_p = h_c$, μm	h_{res} , μm	$h_{e-p} = h_c - h_{\text{res}}$, nm
1	Undeformed AISI 316L sample	3.19 ± 0.05	3.02 ± 0.05	2.93 ± 0.04	0.09 ± 0.01
2	Sample AISI 316L deformed at 30 rpm	2.27 ± 0.05	2.08 ± 0.06	1.93 ± 0.08	0.15 ± 0.04
3	Sample AISI 316L deformed at 300 rpm	2.24 ± 0.12	2.17 ± 0.14	1.95 ± 0.24	0.22 ± 0.11

It can be seen from the table that the value of the parameters h_{\max} , h_c , and h_{res} is the largest for sample 1 and decreases when moving to samples 2 and 3. At the same time, the parameter h_{e-p} experiences an increase in the series 1, 2, 3. A decrease in the parameters h_{\max} , h_c , and h_{res} of the deformed samples compared to the undeformed ones indicates an increase in relaxation properties because of modification of the internal structure of the material (the appearance of dislocation slip bands, their complication, intersection with other grains, etc.). The creation of complex intragranular and intergranular dislocation structures increases the elastic properties of the material in the deformation zone, which leads to an increase in the elastoplastic relaxation of the sample when the load is removed.

The successive growth of the h_{e-p} parameter in the series 1, 2, 3 indicates the complication of the defect structure in the deformed samples compared to undeformed ones. Moreover, the relative velocity of rubbing bodies of 300 rpm creates a more complex defect structure in the sample than that of 30 rpm.

Additional information regarding the specifics of the indentation process can be obtained by analyzing the strain curves, $P(h)$. As an example, Figure 8 shows the “loading-unloading” curves for specimens 1 and 2 at a maximum load of $P_{\max} = 20$ mN (Figure 8a) and $P_{\max} = 400$ mN (Figure 8b). The indentation curves both for undeformed and deformed samples having a fairly smooth running, without “pop-in” or “pop-out” effects. This indicates that the process of deepening the indenter proceeds smoothly, without large jumps or cracks. It is clearly seen that the elastoplastic recovery of the imprint is higher in the deformed sample, correlating with the results of Table 2. At the same time, small zigzags (discrete ‘jumps’) are visible on these curves both at the stage of insertion of the indenter and at the stage of unloading. The effect is more pronounced in sample 2.

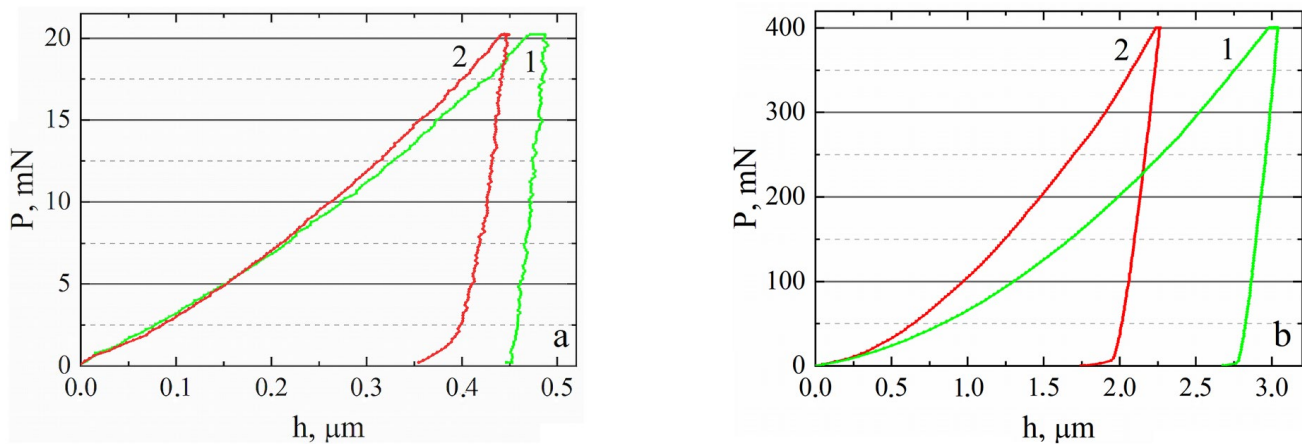


Figure 8. ‘Loading-unloading’ strain curves during nanoindentation with $P_{\max} = 20$ mN (a) and $P_{\max} = 400$ mN (b). Curves 1 correspond to the undeformed specimen and curves 2 to the specimen after 15 h of friction on a cross-section near the friction surface.

In the literature, this effect is widely known and is characterized as a “serration” effect [29,30]. The appearance of the “serrated” effect in different materials is explained by the wave-like nature of the elastoplastic mass transfer in the region of maximum shear stresses under the application of a concentrated load and, in particular, during nanomicroindentation. It has been found on various materials that the tendency of the curves to oscillate (“jagged”) is most pronounced at light loads (<50 mN). As the maximum load increases, the indentation curves become smoother. This pattern is also observed on the AISI 316L samples studied in this work. Comparison of Figure 8a,b clearly shows the difference in the shape of curves obtained at $P_{\max} = 20$ mN and $P_{\max} = 400$ mN.

Considering that, in our experiments, the duration of loading and unloading was the same for all loads (20 s), the indenter penetration rate (v_{in}) increased by a factor of 20 with the transition from the minimum (20 mN) to the maximum load (400 mN). The factor responsible for the increase in the uniformity of the deformation process with increasing v_{in} may be the limited ability of the material to relax the internal stresses that are accumulated during indentation. When a load is applied and removed, the sample feedback consists of a series of successive relaxation displacements, inelastic and elastoplastic transfers of atoms, which manifest themselves in the ‘load-depth’ curve in the form of oscillations (jumps). The faster the rate of application–removal of the load increases, the less time the material has to rearrange the local atomic structure—respectively, the greater the contribution of the translational motion of the indenter, which increases the uniformity of the process and reduces oscillations.

In addition, an increase in the maximum load is accompanied by an increase in the elastoplastic relaxation of the sample (see Figure 8). Thus, at the indentation load $P_{\max} = 20$ mN, the relaxation of undeformed (1) and deformed specimens (2) is 10% and 21%, respectively, whereas at $P_{\max} = 400$ mN it increases to 18% and 25% for specimens (1) and (2), respectively. This effect is due to the creation at a high load of a more developed defect structure consisting of dislocation clusters, sessile dislocations, slip bands, and mutual intersections of intragranular and intergranular dislocations [31,32]. Such a structure has high elastoplastic properties, increasing the feedback of the sample when the load is removed. The results and conclusions of [33] can serve as confirmation of the noted mechanisms. So, Peng et al. studied the microstructure and mechanical properties of AISI 316L steel produced by selective laser melting (SLMed 316L) and then modified by friction stir processing (FSP) technology. It was found that, as a result of such treatment, the microhardness, nanohardness, yield strength, and tensile strength increased markedly. Along with this, the grain size and the total dislocation density decreased, while the geometrically required dislocation density increased. It has been established that the main factors affecting the strength parameters of SLMed 316L are grain sizes and their orientation, density, and interaction of dislocations.

Thus, the performed studies have shown that the microstructural and strength parameters of AISI 316L steel subjected to low friction are sensitive to changes in the relative velocity of rubbing bodies, increasing with the latter. For different velocities (30 rpm and 300 rpm), a general pattern was revealed. First, the friction effect increases the strength and plasticity parameters compared to the initial undeformed sample, and second, their value tends to decrease with a distance from the friction surface to the values of the undeformed sample.

It is worthy of note that the thickness of a layer in which the intensive change of material properties occurs near frictional surfaces in metal-forming processes is also a few tens of microns [34,35], which shows the similarity between the two processes (dry friction and metal forming) at that level.

4. Conclusions

In this work, tribological studies have been carried out concerning the effect of the relative velocity of rubbing bodies on the microstructure and mechanical properties of AISI 316L austenitic steel. It has been shown that low friction of the “metal/metal” type (AISI 316L/St3sp) is capable of introducing noticeable near-surface microstructural and strength changes in AISI 316L steel. The strength parameters (H , E , H/E , and H^3/E^2) increase in the samples subjected to friction compared to the original undeformed sample. It has been established that the maximum changes in all parameters take place near the friction surface (up to 50 μm). The hardness increased from 1.72 GPa for the undeformed sample to 3.5 GPa for the sample subjected to friction for 15 h and Young’s modulus from 107 GPa to 140 GPa, respectively. Relaxation parameters (h_{\max} , h_c , and h_{res}) decrease, while h_{e-p} increases. The changes studied in the present paper successively decrease with distance from the friction surface. The parameters become equal to the values of the undeformed sample at a distance of $t \approx 500$ μm .

It has been shown that the strength and relaxation parameters of the samples deformed by friction at the relative velocity of rubbing bodies of 300 rpm are higher than those of samples subjected to friction at 30 rpm. The process of indentation of all types of samples has proceeded quite smoothly, without sharp jumps or cracks, but at the same time, it has demonstrated a slight step-like deformation, typical for many materials, both at the stage of loading and at the stage of unloading. The manifestation of the “serration” effect in different materials is of a rather general nature and is explained by the wave-like nature of the elastoplastic mass transfer in the region of maximum shear stresses under the application of a concentrated load and, in particular, during nanomicroindentation. The results obtained can be useful in developing materials with high strength and high ductility or wear resistance, as well as in lithographic technologies and memory devices.

Author Contributions: Conceptualization, D.G., S.A. and D.V.; methodology, O.S.; software, C.P.; validation, D.G. and M.V.; resources, M.V.; investigation, C.P. and D.T.; data curation, O.S.; writing—original draft preparation, D.G.; writing—review and editing, D.G., S.A. and M.V.; visualization, D.G. and M.V.; project administration, O.S. All authors have read and agreed to the published version of the manuscript.

Funding: This publication has been supported by the National Agency for Research and Development of the Republic of Moldova under grant No. 20.80009.5007.18, for period from 1 January 2020 to 31 December 2023 and the Serbian Ministry of Science, Technological Development and Innovation, through project No. 451-03-47/2023-01/200156 for period from 1 January 2020 to present.

Data Availability Statement: The data are unavailable.

Acknowledgments: This publication has been supported by the RUDN University Scientific Projects Grant System, project No. 202247-2-000.

Conflicts of Interest: The authors declare no conflict of interest.

References

- Bhushan, B. *Introduction to Tribology*, 2nd ed.; Wiley: New York, NY, USA, 2013; ISBN 978-1-119-94453-9.
- Rojacz, H.; Nevosad, A.; Varga, M. On Wear Mechanisms and Microstructural Changes in Nano-Scratches of Fcc Metals. *Wear* **2023**, 526–527, 204928. [\[CrossRef\]](#)
- Wang, Y.; Zhou, T.; Riemer, O.; Heidhoff, J.; Li, M.; Karpuschewski, B.; Gorb, S.N.; Schaber, C.F. Tribological Mechanism of Micro/Meso/Macroscopic Textured Surfaces under Different Normal Forces, Relative Velocities, and Sliding Directions. *Trib. Int.* **2022**, 176, 107708. [\[CrossRef\]](#)
- Dvoruk, V.I.; Borak, K.V.; Buchko, I.O.; Dobranskiy, S.S. Destruction of Strain Hardened Steel Upon Abrasive Wear. *J. Frict. Wear* **2021**, 42, 178–184. [\[CrossRef\]](#)
- Bowden, F.P.; Leben, L. The Nature of Sliding and the Analysis of Friction. *Proc. R. Soc. Lond.* **1939**, 169, 371–391. [\[CrossRef\]](#)
- Pan, L.; Kwok, C.T.; Lo, K.H. Friction-Stir Processing of AISI 440C High-Carbon Martensitic Stainless Steel for Improving Hardness and Corrosion Resistance. *J. Mater. Process. Technol.* **2020**, 277, 116448. [\[CrossRef\]](#)
- Hajian, M.; Abdollah-zadeh, A.; Rezaei-Nejad, S.S.; Assadi, H.; Hadavi, S.M.M.; Chung, K.; Shokouhimehr, M. Microstructure and Mechanical Properties of Friction Stir Processed AISI 316L Stainless Steel. *Mater. Des.* **2015**, 67, 82–94. [\[CrossRef\]](#)
- Dogan, H.; Findik, F.; Morgul, O. Friction and Wear Behaviour of Implanted AISI 316L SS and Comparison with a Substrate. *Mater. Des.* **2002**, 23, 605–610. [\[CrossRef\]](#)
- Trevisiol, C.; Jourani, A.; Bouvier, S. Effect of Hardness, Microstructure, Normal Load and Abrasive Size on Friction and on Wear Behaviour of 35NCD16 Steel. *Wear* **2017**, 388–389, 101–111. [\[CrossRef\]](#)
- Gain, A.K.; Li, Z.; Zhang, L. Wear mechanism, subsurface structure and nanomechanical properties of additive manufactured Inconel nickel (IN718) alloy. *Wear* **2023**, 523, 204863. [\[CrossRef\]](#)
- Rapoport, L.S. Levels of Plastic Deformation of Layers and Their Connection with the Wear Process. *Frict. Wear* **1989**, 10, 121–131. (In Russian)
- Rapoport, L.S.; Rybakova, L.S. Influence of the Structural State of Surface Layers on Friction and Wear Processes. *Frict. Wear* **1987**, 8, 888–894; 1038–1043. (In Russian)
- Lyamina, E.; Alexandrov, S.; Grabco, D.; Shikimaka, O. An Approach to Prediction of Evolution of Material Properties in the Vicinity of Frictional Interfaces in Metal Forming. *Key. Eng.* **2007**, 345–346, 741–744. [\[CrossRef\]](#)
- Grabco, D.; Alexandrov, S.; Leu, D.; Rahvalov, V.; Shikimaka, O. Behaviour of Ductile Materials Under Friction, Extrusion and Concentrated Load Action. *Mold. J. Phys. Sci.* **2004**, 3, 172–177.
- Grabco, D.; Shikimaka, O.; Alexandrov, S.; Harea, E.E.; Mirgorodskaya, I.Y.; Danitsa, Z.N. Evolution of Change in Microstructure of Material as It Moves Farther from Frictional Contact Surface under Conditions of Severe Plastic Deformation. In Proceedings of the XVIII St.-Petersburg Readings on Problems of Strength and Crystal Growth, Saint-Peterburg, Russia, 21–24 October 2008; pp. 152–154, Part 1.
- Aleksandrov, S.E.; Grabko, D.Z.; Shikimaka, O.A. The Determination of the Thickness of a Layer of Intensive Deformations in the Vicinity of the Friction Surface in Metal Forming Processes. *J. Mach. Manuf. Reliab.* **2009**, 38, 277–282. [\[CrossRef\]](#)
- Grabco, D.; Pyrtsac, C.; Topal, D.; Shikimaka, O. Effect of Friction on the Micromechanical Properties of AISI 316L Austenitic Steel. *J. Eng. Sci.* **2021**, 28, 34–43. [\[CrossRef\]](#) [\[PubMed\]](#)
- Xue, Z.; Zhu, Z.; Zhu, D.; Li, T.; Yang, C. High-speed Electrodeposition of Bright Cu with Excellent Mechanical Properties Utilizing Friction of Hard Particles. *J. Mat. Sci.* **2023**, 58, 3752–3767. [\[CrossRef\]](#)
- Oliver, W.C.; Pharr, G.M. An Improved Technique for Determining Hardness and Elastic Modulus Using Load and Displacement Sensing Indentation Experiments. *J. Mater. Res.* **1992**, 7, 1564–1583. [\[CrossRef\]](#)
- Golovin, Y.I. Nanoindentation and Mechanical Properties of Solids in Submicrovolumes, Thin Surface Layers and Films: A Review. *Phys. Solid State* **2008**, 50, 2113–2142. [\[CrossRef\]](#)

21. ISO 14577-1:2015(en); Metallic Materials-Instrumented Indentation Test for Hardness and Materials Parameters-Part 1: Test method. International Organization for Standardization: Geneva, Switzerland, 2002.
22. Lim, Y.Y.; Chaudhri, M.M. The Effect of the Indenter Load on the Nanohardness of Ductile Metals: An Experimental Study on Polycrystalline Work-Hardened and Annealed Oxygen-Free Copper. *Phil. Mag. A* **1999**, *79*, 2979–3000. [[CrossRef](#)]
23. Zong, Z.; Soboyejo, W. Indentation Size Effects in Face Centered Cubic Single Crystal Thin Films. *Mater. Sci. Eng. A* **2005**, *404*, 281–290. [[CrossRef](#)]
24. Leyland, A.; Matthews, A. On the Significance of the H/E Ratio in Wear Control: A Nanocomposite Coating Approach to Optimised Tribological Behaviour. *Wear* **2000**, *246*, 1–11. [[CrossRef](#)]
25. Musil, J.; Kunc, F.; Zeman, H.; Poláková, H. Relationships between Hardness, Young's Modulus and Elastic Recovery in Hard Nanocomposite Coatings. *Surf. Coat. Techn.* **2002**, *154*, 304–313. [[CrossRef](#)]
26. Ren, Y.; Liang, L.; Shan, Q.; Cai, A.; Du, J.; Huang, Q.; Liu, S.; Yang, X.; Tian, Y.; Wu, H. Effect of Volumetric Energy Density on Microstructure and Tribological Properties of FeCoNiCuAl High-entropy Alloy Produced by Laser Powder Bed Fusion. *Virtual Phys. Prototyp.* **2020**, *15* (Suppl. S1), 543–554. [[CrossRef](#)]
27. Jang, J. Estimation of Residual Stress by Instrumented Indentation: A review. *J. Ceram. Process. Res.* **2009**, *10*, 391–400.
28. Grabco, D.; Shikimaka, O.; Pyrtsac, C.; Barbos, Z.; Popa, M.; Prisacaru, A.; Vilotic, D.; Vilotic, M.; Alexandrov, S. Nano- and Micromechanical Parameters of AISI 316L Steel. *Surf. Eng. Appl. Electr.* **2020**, *56*, 719–726. [[CrossRef](#)]
29. Zuev, L.B.; Barannikova, S.A.; Zarikovskaya, N.V.; Zykov, I.Y. Phenomenology of Wave Processes in a Localized Plastic Flow. *Phys. Solid State* **2001**, *43*, 1483–1487. [[CrossRef](#)]
30. Dey, A.; Chakraborty, R.; Mukhopadhyay, A.K. Enhancement in Nanohardness of Soda–Lime–Silica Glass. *J. Non. Cryst. Solids.* **2011**, *357*, 2934–2940. [[CrossRef](#)]
31. Grabco, D.; Shikimaka, O.; Harea, E. Translation–Rotation Plasticity as Basic Mechanism of Plastic Deformation in Macro-, Micro- and Nanoindentation Processes. *J. Phys. D Appl. Phys.* **2008**, *41*, 074016. [[CrossRef](#)]
32. Grabco, D.; Pyrtsac, C.; Shikimaka, O. Influence of substrate type on deformation specificity of soft film/hard substrate coated systems under nanomicroindentation. *Phil. Mag.* **2023**, *103*, 1146–1176. [[CrossRef](#)]
33. Peng, P.; Wang, K.; Wang, W.; Han, P.; Zhang, T.; Liu, O.; Zhang, S.; Wang, H.; Qiao, K.; Liu, J. Relationship between Microstructure and Mechanical Properties of Friction Stir Processed AISI 316L Steel Produced by Selective Laser Melting. *Mater. Charact.* **2020**, *163*, 110283. [[CrossRef](#)]
34. Alexandrov, S.; Jeng, Y.-R.; Hwang, Y.-M. Generation of a Fine Grain Layer in the Vicinity of Frictional Interfaces in Direct Extrusion of AZ31 Alloy. *ASME J. Manuf. Sci. Eng.* **2015**, *137*, 051003. [[CrossRef](#)]
35. Alexandrov, S.; Jeng, Y.-R.; Kuo, C.-Y.; Chen, C.-Y. Towards the Theoretical/Experimental Description of the Evolution of Material Properties at Frictional Interfaces in Metal Forming Processes. *Trib. Int.* **2022**, *171*, 107518. [[CrossRef](#)]

Disclaimer/Publisher's Note: The statements, opinions and data contained in all publications are solely those of the individual author(s) and contributor(s) and not of MDPI and/or the editor(s). MDPI and/or the editor(s) disclaim responsibility for any injury to people or property resulting from any ideas, methods, instructions or products referred to in the content.